# STREAMLINE SWALLOWING
# BY LAMINAR BOUNDARY LAYERS
# IN HYPERSONIC FLOW

A. W. Mayne, Jr. and J. C. Adams, Jr.

ARO, Inc.

## March 1971

## VON KÁRMÁN GAS DYNAMICS FACILITY
## ARNOLD ENGINEERING DEVELOPMENT CENTER
## AIR FORCE SYSTEMS COMMAND
## ARNOLD AIR FORCE STATION, TENNESSEE

# NOTICES

# STREAMLINE SWALLOWING
# BY LAMINAR BOUNDARY LAYERS
# IN HYPERSONIC FLOW

A. W. Mayne, Jr. and J. C. Adams, Jr.

ARO, Inc.

# FOREWORD

The work reported herein was sponsored by the Arnold Engineering Development Center (AEDC), Air Force Systems Command (AFSC), under Program Element 62201F, Project 8953, Task 03.

The results of the research presented were obtained by ARO, Inc. (a subsidiary of Sverdrup & Parcel and Associates, Inc.), contract operator of AEDC, AFSC, Arnold Air Force Station, Tennessee, under Contract F40600-71-C-0002. The work was performed during the period from September 1969 through June 1970 under ARO Project No. VW5006, and the manuscript was submitted for publication on December 10, 1970.

The authors wish to thank D. H. Wurst, M. Brown, and B. J. Clayton of ARO, Inc., for their help in performing the numerical calculations reported herein. Acknowledgment and appreciation is also extended to R. T. Davis, Professor of Engineering Mechanics at Virginia Polytechnic Institute, for providing the authors with an updated copy of his viscous shock layer digital computer program. The fully viscous shock layer results presented herein have been taken from calculations performed by E. O. Marchand of ARO, Inc.

Portions of the low Reynolds number results in this report were presented in a paper by J. C. Adams, Jr. and A. W. Mayne, Jr., entitled "Analysis of the Laminar Boundary Layer on a Hyperboloid in Hypersonic Flow Including Boundary-Layer Swallowing of the Bow-Shock-Generated Rotational Inviscid Entropy Layer," given at the Sixth Southeastern Seminar on Thermal Sciences at Raleigh, North Carolina, on April 13 and 14, 1970.

This technical report has been reviewed and is approved.

David C. Reynolds
Captain, USAF
Research and Development
   Division
Directorate of Technology

Harry L. Maynard
Colonel, USAF
Director of Technology

## ABSTRACT

Flow over a cold-wall, 22.5-deg asymptotic half-angle hyperboloid at a free-stream Mach number of 10 and free-stream Reynolds numbers (based on nose radius) of 400, 4000, and 40,000 is considered. Numerical results from a streamline-swallowing, nonsimilar, laminar, boundary-layer analysis are compared with results from classical boundary-layer theory, second-order boundary-layer theory, and a fully viscous shock-layer analysis; the results of the latter are used as a standard of comparison. The major improvement effected by the streamline-swallowing analysis is the inclusion of shock curvature effects on the boundary conditions applied along the outer edge of the boundary layer. Results from the streamline-swallowing boundary-layer analysis agree well with the results of the fully viscous shock-layer analysis, but the classical boundary layer and the second-order boundary-layer results give poor agreement. Reasons for the success of the one method and the failure of the other two are discussed.

# CONTENTS

## APPENDIX
## ILLUSTRATIONS

## NOMENCLATURE

| | |
|---|---|
| $C_{f_\infty}$ | Local skin-friction coefficient = $2\tau_w / \rho_\infty U_\infty^2$ |
| $c_p$ | Specific heat at constant pressure |
| $M_\infty$ | Free-stream Mach number |
| $p$ | Pressure |
| $p_e$ | Pressure at outer edge of boundary layer |
| $p_o$ | Free-stream normal shock pitot pressure |
| $\dot{q}_w$ | Wall heat flux |
| $Re_{\infty, r_n}$ | Reynolds number based on nose radius and free-stream conditions = $\rho_\infty U_\infty r_n / \mu_\infty$ |
| $r$ | Radius |
| $r_n$ | Nose radius of curvature |
| $St_\infty$ | Stanton number based on free-stream conditions = $\dfrac{\dot{q}_w}{\rho_\infty U_\infty c_p (T_o - T_{wall})}$ |
| $s$ | Surface distance measured from stagnation point |
| $T$ | Temperature |
| $T_e$ | Temperature at outer edge of boundary layer |

vi

| | |
|---|---|
| $T_O$ | Free-stream stagnation temperature |
| $T_{wall}$ | Wall temperature |
| $T_\infty$ | Free-stream temperature |
| $U_\infty$ | Free-stream velocity |
| $u$ | Tangential velocity |
| $u_e$ | Tangential velocity at outer edge of boundary layer |
| $y$ | Distance normal to surface |
| $y_e$ | Normal distance from surface to edge of boundary layer |
| $y_s$ | Radius of shock for mass balance |
| $\mu_\infty$ | Free-stream viscosity |
| $\rho$ | Density |
| $\rho_\infty$ | Free-stream density |
| $\tau_w$ | Wall shear stress |

# SECTION I
# INTRODUCTION

For hypersonic flight in the earth's atmosphere, heat transfer and other considerations require blunting of the nose or leading edge of the flight vehicle. The entropy layer caused by the curved bow shock associated with nose blunting produces a rotational inviscid external stream into which the boundary layer grows. The flow entering the boundary layer is initially the hot, high entropy gas which has been stagnated, or nearly so, in the region of the bow shock. As the gas flows over the body, all of the high entropy gas initially processed by the bow shock, which is termed the entropy layer, eventually is entrained, or swallowed, by the boundary layer. Additional gas subsequently added to the boundary layer is a cooler, lower entropy gas which has traversed only the weaker portions of the shock wave.

As first pointed out by Ferri and Libby (Ref. 1) the interaction between the rotational external flow and the boundary layer may in some instances invalidate the classical boundary-layer approach. This interaction effect becomes important when the vorticity of the external stream is of the same order as the average vorticity in the boundary layer (Ref. 2). These conditions may exist, for example, in the combination of low Reynolds number (low boundary-layer vorticity) and high Mach number (high external stream vorticity because of the highly curved shock). As the Reynolds number is increased, the effect of the external vorticity on the boundary-layer velocity and temperature profiles is lessened. Therefore, the results of a classical boundary-layer analysis may closely approximate the true physical situation provided the calculations are carried out in a consistent manner and account for the variation of the boundary-layer outer-edge conditions caused by the curved shock. Such analyses have been performed by Zakkay and Krause (Ref. 3), Wilson (Ref. 4), Rotta and Zakkay (Ref. 5), Murzinov (Ref. 6), and Levine (Ref. 7). These references clearly reveal the necessity of including entropy-layer swallowing in blunt body boundary-layer analyses for accurate predictions of measurable quantities such as wall heat transfer and skin friction.

An alternate approach to this interaction problem involves second-order boundary-layer theory as derived by Van Dyke (Ref. 8). Basically, Van Dyke's approach involves solving first- and second-order boundary-layer equations which are found from the complete Navier-Stokes equations by an expansion in inverse powers of the square-root of a Reynolds number. The expansion procedure used is the method of inner and outer expansions and results in replacing the Navier-Stokes equations by two

separate sets of equations: one set which is valid in the outer inviscid region and another set which is valid in the inner viscous (boundary-layer) region. By using Van Dyke's perturbation procedure the resulting second-order boundary-layer equations are linear and can be subdivided to exhibit several second-order boundary-layer effects: displacement, external vorticity, longitudinal curvature, transverse curvature, slip, and temperature jump. In this approach the above effects are treated as second-order perturbations which are added to the first-order results. However, as shown by Adams (Ref. 9), one should properly interpret second-order vorticity and displacement as a combined effect (vorticity-displacement interaction) so that the separate influence of external vorticity connot be assessed using second-order boundary-layer theory. Numerical solutions to the second-order boundary-layer equations have been presented by Davis and Flügge-Lotz (Ref. 10), Fannelop and Flügge-Lotz (Ref. 11), Maslen (Ref. 12), Marchand, Lewis, and Davis (Ref. 13), Lewis (Ref. 14), and Adams (Ref. 9).

The work by Davis and Flügge-Lotz (Ref. 10) represents the first attempt at numerical solution of the second-order boundary-layer equations in regions removed from the blunt nose. One of the bodies considered in their analysis was a 22.5-deg asymptotic half-angle hyperboloid at hypersonic flow conditions. This particular combination of body and flow exhibits strong growth of vorticity-displacement interaction as the computation proceeds downstream, and the indication is that the effect of vorticity-displacement interaction becomes a first-order effect at distances far downstream from the nose. As discussed in Refs. 9, 13, and 14, second-order boundary-layer theory does not properly take into account the effect of strong vorticity-displacement interaction such as discussed above for the hyperboloid flow. The important question remains as to the limits of validity for second-order boundary-layer vorticity-displacement interaction.

Because of the difficulties mentioned above with second-order boundary-layer theory, it is desirable to seek an alternative approach to the blunt-body problem in hypersonic flow. The most appealing method is one originally suggested by Cheng (Ref. 15) for solving a set of equations that is valid throughout the entire shock layer. Davis and Flügge-Lotz (Ref. 10) derived a more complete set of equations which contains all of the terms in the Navier-Stokes equations which contribute to second-order boundary-layer theory plus those which arise to second order in the outer inviscid flow. By making the thin shock-layer approximation on the resulting momentum equation normal to the body surface, these equations are reduced by Davis (Ref. 16) to a set of equations which is parabolic in form. Davis includes both shock and

body slip in his treatment and numerically integrates the equations using an implicit finite-difference technique very similar to that of Flügge-Lotz and Blottner (Ref. 17). Since this approach considers the entire shock layer to be viscous with the shock standoff determined as part of the solution, none of the matching problems associated with first- and second-order boundary-layer analyses is present. However, because of the choice of coordinate systems, the thin viscous shock-layer analysis of Davis (Ref. 16) is restricted to treatment of analytic bodies of revolution. In practice this means that a body shape such as a sphere-cone cannot be analyzed using the Davis viscous shock-layer approach because of the discontinuity in body curvature at the sphere-cone junction.

Given a body and flow condition, the aerodynamicist is faced with the choice of an appropriate analysis technique — be it boundary layer, viscous shock layer, or other approach. The present report will concentrate on assessing the applicability of classical boundary-layer theory modified to include the effects of variation in the boundary-layer outer-edge conditions caused by the curved bow shock, i.e., inclusion of streamline swallowing. This assessment is based on comparisons of results from a classical boundary-layer approach (neglecting streamline swallowing), second-order boundary-layer theory, and a boundary-layer treatment including streamline swallowing with results from a fully viscous shock-layer treatment. The results compared are for the case of Mach number 10 flow over a 22.5-deg asymptotic half-angle hyperboloid over a large range of Reynolds numbers.

## SECTION II
## BODY AND FLOW CONDITIONS

The present work is devoted to the analysis of flow over a 22.5-deg asymptotic half-angle hyperboloid, which is identical to the body considered by Adams (Ref. 9) and Davis (Ref. 16). A body 20 nose radii long, measured along the body surface, has been considered. Three free-stream conditions have been analytically investigated: the Mach number was 10 and the free-stream temperature was 100°K for each condition; however, free-stream Reynolds numbers (based on nose radius) of 400, 4000, and 40,000 have been considered. The wall-to-stagnation temperature ratio has been held constant at 0.2, the ratio of specific heats was 1.4, and a constant Prandtl number of 0.7 has been assumed. The gas has been assumed to be thermally and calorically perfect air with the viscosity following the Sutherland law. The angle of attack of the body relative to the free stream was zero. It might be

noted that the lowest Reynolds number condition corresponds to that considered by Adams (Ref. 9) and Davis (Ref. 16).

The above flow conditions are such that at the lowest Reynolds number viscous effects are significant in almost the entire region between the body and the shock, but at the highest Reynolds number a relatively thin boundary layer exists. Swallowing of the bow-shock-generated entropy layer by the boundary layer is significant for each of the Reynolds numbers, although the effect is most pronounced at the lowest Reynolds number condition. Only the cold-wall condition has been considered since that is usually the case of most interest with respect to testing in hypersonic facilities.

# SECTION III
# PRESENT ANALYSIS

The theory and numerical scheme used in obtaining the present results are based, in part, on the work of Patankar and Spalding (Refs. 18 and 19). In this approach the classical boundary-layer equations, with the addition of the transverse curvature terms, are expressed in a normalized von Mises coordinate system and solved by using a marching, implicit finite-difference procedure. Although the primary use of the work of Patankar and Spalding has been in the analysis of turbulent boundary layers, the present application is concerned exclusively with laminar boundary layers. Further details concerning the digital computer code and its application are given in a later paragraph.

As stated previously, an item of primary interest in this report is the effect on computed boundary-layer results of an improved method of determining the boundary-layer outer-edge conditions for cases of flow over blunt bodies: namely, the consideration of the effects of streamline swallowing. The specification of the conditions along the outer edge of the boundary layer is reasonably straightforward for bodies such as flat plates and sharp cones; however, for the case of a blunt body the problem is more complex. The simplest and, therefore, the most commonly employed method is to first obtain a pressure distribution over the body of interest from an inviscid method of characteristics solution or Newtonian theory. Free-stream stagnation conditions behind a normal shock are then determined, and the local flow conditions along the boundary-layer edge are found by isentropically expanding from these stagnation conditions to the known local pressure, thus treating the boundary-layer edge as an isentropic surface. This

method is satisfactory for the forward portion of a blunt body; however, as the flow proceeds along the body and the boundary layer grows because of entrainment of mass, the high entropy portion of the flow which crossed the essentially normal portion of the bow shock is swallowed by the boundary layer. The flow along the edge of the boundary layer on the aft portions of the body will then have passed through an oblique part of the bow shock and will be in a different state than had it passed through a normal shock (Fig. 1, Appendix).

Assuming the pressure along the outer edge of the boundary layer on a blunt body to have the inviscid surface value,* the determination of the local edge flow conditions may be improved by taking into consideration the inclination of the bow shock where the flow crossed the shock. The point at which the flow along the edge of the boundary layer crossed the shock can be determined by matching the mass flow in the boundary layer at a given location to the free-stream mass flow in a cylinder with radius extending out to the location to be determined. Referring again to Fig. 1, this may be expressed as

$$\rho_\infty U_\infty \pi y_s^2 = \int_0^{y_e} 2\pi r \, \rho u \, dy$$

After $y_s$ is found, the shock inclination at that point can be determined and the flow conditions along the boundary layer at the corresponding body location can be computed by crossing the oblique shock at $y_s$ with the free-stream flow and allowing that flow to expand isentropically to the known local boundary-layer edge pressure. Naturally, a swallowing analysis such as described above requires that the shape of the bow shock be known in addition to the body surface pressure. In the present calculations these data were obtained from the blunt body and method of characteristics solution of Inouye, Rakich, and Lomax (Ref. 20).

When streamline swallowing is being considered, the definition of the outer edge of the boundary layer must be reconsidered. This is necessary because the velocity and temperature gradients are not zero at the outer edge of the boundary layer, but have values associated with the inviscid flow field. This is the result of the combination of the streamline swallowing and the use of the nonsimilar boundary-layer equations. To treat this situation the boundary-layer thickness may be

---

*This assumption should be valid as long as the pressure gradient normal to the body surface is small.

redefined in terms of the total enthalpy, since the gradient of this quantity does go to zero at the boundary-layer edge. This approach, proposed by Levine (Ref. 7), was used in obtaining the results presented herein which include the effects of streamline swallowing. In particular, the region treated by the boundary-layer equations was adjusted such that $y_e$ was equal to 1.1 times the value of y where

$$\frac{T + u^2/2c_p - T_{wall}}{T_o - T_{wall}} = 0.999$$

With the outer-edge boundary condition determined by the streamline-swallowing technique given above, the numerical computation proceeds downstream using the marching, implicit finite-difference method of solution discussed previously (Refs. 18 and 19). Note that this approach properly considers the nonsimilar growth of the boundary layer along the body. In the present analysis, no-slip boundary conditions are applied at the body surface with respect to velocity and temperature.

To solve parabolic partial differential equations, such as the boundary-layer equations treated herein, it is necessary to specify both the boundary conditions on the dependent variables and initial values of the dependent variables in the cross-stream direction. Experience has shown that any choice of initial profiles which is not entirely unreasonable can be used with a negligible effect on the downstream results if the computations are begun near the leading edge of a sharp body or the stagnation point of a blunt body. This experience has been used to obtain laminar boundary-layer solutions in the vicinity of the stagnation point of a blunt body by beginning the solution near the stagnation point with assumed profiles and using a number of very small steps in the streamwise direction.

The computer program used in the present work is written in FORTRAN 63 for use on a CDC 1604-B digital computer and is essentially a highly modified version of the code originally devised by Patankar and Spalding (Ref. 19). This program, formulated by Mayne and Dyer (Ref. 21), is capable of treating nonsimilar laminar or turbulent boundary layers over both sharp- and blunt-nosed two-dimensional or axisymmetric bodies in a compressible, perfect gas flow. For turbulent boundary-layer flows, an eddy viscosity approach based on the mixing-length concept is used in conjunction with a step instantaneous transition from laminar to turbulent flow. In addition, the program is capable of treating homogeneous arbitrarily prescribed surface mass transfer into either a laminar or turbulent boundary layer. For blunt-nosed bodies in supersonic or hypersonic flows, the swallowing treatment

discussed in this report may be applied at the discretion of the user. The Mayne and Dyer formalism embodies a number of significant modifications and extensions to the basic technique of Patankar and Spalding. These include elimination of the Couette flow analysis at the body surface and the so-called slip-value scheme in favor of applying the basic finite-difference scheme across the entire boundary layer. The introduction of a variable cross-stream step size which is smaller near the wall than at the outer edge of the boundary layer yields accurate solutions while still permitting the computations to proceed efficiently. Because of the implicit nature of the finite-difference scheme, no numerical stability problems are to be expected from this approach; experience has indicated this to be true.

It should be noted that the results of the fully viscous shock-layer calculations presented herein are based on the assumptions of no wall or shock slip and a simple Rankine-Hugoniot shock wave. This has been done to be consistent with the calculations made using the boundary layer with streamline-swallowing approach, although these neglected slip effects are not large at even the lowest Reynolds number condition, as shown by Davis (Ref. 16). All of the fully viscous shock-layer calculations have been iterated at least twice to remove the thin shock-layer approximation on the normal momentum equation. See Davis (Ref. 16) for a complete discussion of this point.

## SECTION IV
## RESULTS AND DISCUSSION

Numerical results from the present investigation are presented in Figs. 2 through 18. At this point the reader should refer again to Fig. 1 for the nomenclature to be used relative to the body geometry. Generally, no results are presented for values of $s/r_n < 1.0$, because the effects of streamline swallowing are not significant near the stagnation point.

Figure 2 shows the thickness of the boundary layer (based on the streamline-swallowing analysis), the fully viscous shock-layer shock location, and a completely inviscid flow shock location for the three conditions considered. As the Reynolds number increases, the shock location determined by the fully viscous shock layer approaches that which is calculated by the inviscid method-of-characteristics solution. At the lowest Reynolds number considered the boundary layer (based on the streamline-swallowing analysis) can be seen to fill most of the region between the body and the inviscid shock over the entire body and even to somewhat exceed this over the forward portion of the body. As the

Reynolds number increases, the boundary-layer thickness decreases, and at the highest Reynolds number the boundary layer fills only about 10 percent of the region between the body and the shock.

Figure 3 shows the Stanton number along the body for the $Re_{\infty, r_n} = 400$ condition. Adopting the fully viscous shock-layer approach to be the most correct treatment of the problem at hand, Fig. 3 shows that the boundary-layer treatment, including streamline swallowing, is in good agreement with the fully viscous shock layer. The boundary-layer results which neglect streamline swallowing, i. e., classical boundary-layer results, are some 20 percent below the fully viscous shock-layer results over the entire body, whereas the results of the second-order boundary-layer analysis by Adams (Ref. 9) vary from 10 to 100 percent above the fully viscous shock-layer results. To explain this discrepancy, Fig. 4 shows the increment in local Stanton number according to second-order boundary-layer theory (Ref. 9) and reveals the strong vorticity-displacement interaction which is by far the dominant second-order effect. As discussed in Ref. 9, second-order boundary-layer theory is not applicable under conditions where the second-order increment becomes of the same magnitude as classical first-order boundary-layer results (compare Figs. 3 and 4 at $s/r_n = 20$). Note that transverse curvature acts to increase surface heat transfer over the entire body, as shown in Fig. 4. Both the analysis by Davis (Ref. 16) and the present modified boundary-layer treatment properly include the transverse curvature terms in the governing equations of motion. As can be seen from Fig. 4, the influence of longitudinal curvature is negligible in regions away from the nose of the body.

Figs. 5 and 6 show the Stanton number distributions over the body for the $Re_{\infty, r_n} = 4000$ and $Re_{\infty, r_n} = 40,000$ conditions, respectively. In both cases the results of the boundary-layer treatment with streamline swallowing agree well with the fully viscous shock-layer results. The classical boundary-layer results consistently fall below the fully viscous shock-layer results, although the discrepancy can be seen to decrease with increasing Reynolds number.

With respect to skin friction along the body, as reflected in the skin-friction coefficient, Fig. 7 shows that for the $Re_{\infty, r_n} = 400$ condition the present boundary-layer treatment, including streamline swallowing, is in good agreement with the fully viscous shock-layer results over the entire body. The second-order boundary-layer prediction is over 100 percent in error for $s/r_n > 10.0$, relative to the fully viscous shock layer. Reference to Fig. 8 shows this failure of second-order boundary-layer theory to be caused by the same vorticity-displacement interaction

discussed previously in connection with the heat-transfer results. Note that Fig. 8 reveals the influence of all other second-order effects to be negligible for the present case. The good agreement between the fully viscous shock layer and the present boundary layer, including entropy swallowing, as shown in Fig. 7, indicates that the present approach is indeed applicable in treating the boundary-layer-inviscid entropy layer interaction problem.

Generally speaking, as the Reynolds number is increased, the results of second-order boundary-layer theory may be expected to show better agreement with the results of the fully viscous shock layer and · boundary layer with streamline swallowing over the length of body considered herein. Were a longer body considered, however, the second- · order boundary-layer results would again become invalid as the vorticity-displacement interaction becomes significant. As discussed by Adams (Ref. 9), this is caused by the nature of the asymptotic matching conditions between the inner and outer flow fields in the second-order perturbation-type analysis.

Figures 9 and 10 show the skin-friction coefficient distribution over the body for the $Re_{\infty, r_n}$ = 4000 and $Re_{\infty, r_n}$ = 40,000 conditions, respectively. Again, the results of the boundary-layer treatment with streamline swallowing agree well with the fully viscous shock-layer results. The results of classical boundary-layer theory consistently fall below the fully viscous shock-layer results, with a 25-percent difference existing at the end of the body ($s/r_n$ = 20) for even the highest Reynolds number case. It has been a general experience that streamline-swallowing effects are larger on skin-friction results than on heat-transfer results, as is the case in this work.

Previous hypersonic flow studies at the von Kármán Gas Dynamics Facility of AEDC (Refs. 22 and 23) have indicated experimentally a large viscous-induced drag increment at zero lift, which cannot be fully explained using classical boundary-layer theory. As can be seen from Figs. 7, 9, and 10, the boundary-layer skin-friction computation without streamline swallowing lies up to 40 percent below the results of fully viscous shock layer and the boundary layer including streamline swallowing. The viscous-induced drag increment discrepancy may, therefore, be attributable to the interaction between the boundary layer and the entropy layer. Unpublished comparisons between experimental and computed viscous drag, including streamline swallowing in the analysis, indicate good agreement and suggest that a boundary-layer analysis must include streamline swallowing to properly account for the viscous-inviscid interaction.

9

Figures 11 and 12 show velocity and temperature profiles, respectively, at two locations along the body for $Re_{\infty, r_n}$ = 400. Good agreement exists between the results of the boundary-layer treatment including streamline swallowing and those determined using the fully viscous shock-layer method. The classical boundary-layer results shown in these two figures are radically different from the other results in both magnitude and character and demonstrate the unsuitability of classical boundary-layer theory for the treatment of this problem.

Figures 13 and 14 show velocity and temperature profiles, respectively, for $Re_{\infty, r_n}$ = 40,000. For this condition where the boundary layer is thin relative to the shock layer there is excellent agreement between both the velocity and temperature profiles computed by the boundary layer with streamline swallowing and by the fully viscous shock-layer method.

Figures 15 and 16 show the development of the boundary-layer outer-edge conditions when streamline swallowing is considered. Figure 15 shows the variation of the edge velocity, and Fig. 16 shows the variation of the edge temperature. Data are shown in each figure for each of the three Reynolds number conditions considered here and for a condition, indicated by $Re_{\infty, r_n}$ = $\infty$, which corresponds to neglecting the streamline-swallowing effects altogether. The $Re_{\infty, r_n}$ = $\infty$ condition may be termed the isentropic body-wetted streamline case, which corresponds to the classical boundary-layer treatment. Also indicated are the limiting values of the edge conditions which would exist on a 22.5-deg half-angle sharp cone. The edge conditions which would prevail if the streamline swallowing were neglected approach limiting values which are quite different from the sharp cone limits which the edge conditions approach when streamline swallowing is considered. The isentropic body-wetted streamline velocity approaches a value 30 percent below the sharp cone limit (Fig. 15) and the corresponding temperature approaches a value which is almost three times the sharp cone limit (Fig. 16). When streamline swallowing is considered, the edge conditions approach the sharp cone limit as flow proceeds along the body with the rate at which the sharp cone limits are approached increasing with decreasing Reynolds number.

An interesting point arises when considering both the boundary-layer outer-edge conditions and the profile data previously discussed. It can be seen in Figs. 11, 12, 13, and 14 that the boundary-layer profiles have significant gradients at the outer edge of the boundary layer, except for the $Re_{\infty, r_n}$ = 400 condition at $s/r_n$ = 20. This is because the

interaction of the nonsimilar boundary layer with the inviscid entropy layer produces gradients near the outer edge of the boundary layer. For the $Re_{\infty, r_n}$ = 400 condition at $s/r_n$ = 20, however, the boundary layer has essentially swallowed the inviscid entropy layer generated by the bow shock. This may be seen in Figs. 15 and 16 where the outer-edge velocity and temperature approach the sharp cone limit at $s/r_n$ = 20 for $Re_{\infty, r_n}$ = 400. Examination of Figs. 11 through 14 reveals the physical behavior of a boundary layer growing into a rotational inviscid stream which contains gradients in its fluid dynamic-thermodynamic properties.

Figure 17 shows the inviscid surface pressure distribution determined using the blunt body and method-of-characteristics solution of Inouye, Rakich, and Lomax (Ref. 20). This is the surface pressure distribution which was used in the calculations of the boundary layer with streamline swallowing. Also shown in Fig. 17 is the limiting value of the surface pressure on a 22.5-deg half-angle sharp cone. Even at the end of the body considered here the surface pressure is still some 7-percent greater than the limiting sharp cone value. Because of this it would, of course, be impossible for the boundary-layer outer-edge boundary conditions to reach the sharp cone limiting values on the body considered.

One may well ask what is the importance of including the viscous-induced pressure in the present analysis. As shown in the upper part of Fig. 17, the fully viscous shock-layer surface pressure is some 5 to 8 percent higher than the inviscid characteristics surface pressure for the lowest Reynolds number condition considered, and this difference decreases with increasing Reynolds number. No attempt has been made in the present analysis to account for the so-called boundary-layer displacement interaction with the inviscid flow which will in turn produce a displacement-induced pressure increase. Levine (Ref. 7) presents a method which can be used to account for the displacement interaction while simultaneously including the streamline-swallowing interaction. It would be of interest to incorporate Levine's approach into the present method and assess the importance of displacement interaction. However, the present results indicate that the entropy interaction through the swallowing process is the dominant effect which must be included in blunt body boundary-layer analyses under hypersonic conditions.

Another important question concerns the normal pressure gradient across the shock layer. As shown by Fig. 18, which is for the body location $s/r_n$ = 15, the pressure ratio remains almost constant across

the shock layer for each of the three Reynolds' number conditions con-
sidered. Hence, the assumption of constant pressure at the inviscid
surface value is reasonable. However, near the nose of the body the
normal pressure gradient is not zero; e. g., the inviscid surface pres-
sure is 0.86 times the pressure immediately behind the shock for the
location $s/r_n$ = 5. Thus, in the nose region of the body the present
analysis is not strictly correct in that the normal pressure gradient is
not accounted for. This omission of the normal pressure gradient in
the nose region appears to have little influence on the downstream
results, as might be expected because of the parabolic form of the
governing boundary-layer equations.

# SECTION V
## SUMMARY AND CONCLUSIONS

The results presented herein have shown the validity of applying a
streamline-swallowing boundary-layer analysis to hypersonic flow over
a blunt body at conditions for which neither a classical boundary-layer
approach nor second-order boundary-layer theory is suitable. The
validity of the results of the three methods has been determined by com-
parison with results obtained by the method of Davis (Ref. 16) using a
fully viscous shock-layer analysis. With respect to both surface-
measurable quantities (heat flux and skin-friction) and profile data, the
streamline-swallowing boundary-layer analysis agrees well with the
results of the fully viscous shock-layer analysis, but the classical
boundary-layer and the second-order boundary-layer results are in
poor agreement, especially at the lowest Reynolds number considered.

The failure of the classical boundary-layer treatment is caused by
the lack of consideration of the shock curvature effects on the boundary
conditions along the outer edge of the boundary layer; the second-order
boundary-layer theory is not applicable because of the very large second-
order vorticity-displacement interaction effect which invalidates the
theory.

For the lowest Reynolds number situation considered, there exists
a thick boundary layer over the entire surface of the body. For this
case the streamline-swallowing effects were shown to be significant
over the whole body. At the higher Reynolds number conditions, with
resultant thinner boundary layers, the streamline-swallowing effects
are still significant, although they begin relatively farther down the body
and persist for a longer distance on the body.

The use of a streamline-swallowing boundary-layer analysis in the present work has yielded good results for a situation in which other boundary-layer methods were inadequate, without requiring a fully viscous shock-layer treatment of the problem, although the latter method does indeed provide a more accurate analysis of the situation. For high density hypersonic flows over blunt bodies with thin boundary layers the authors recommend the streamline-swallowing boundary-layer analysis as the most efficient calculation technique because of the grid-spacing considerations and the lack of viscous-inviscid interaction other than the streamline-swallowing effect. Furthermore, the authors believe the use of a streamline-swallowing approach in conjunction with a nonsimilar boundary-layer integration technique to be especially imperative if one is interested in accurate analysis of compressible turbulent boundary layers on blunt-nosed bodies under cold-wall hypersonic conditions.

## REFERENCES

1. Ferri, A. and Libby, P. A. "Note on the Interaction between the Boundary Layer and the Inviscid Flow." J. Aero. Sci., Vol. 21, 1954, p. 130.

2. Ferri, A. "Some Heat Transfer Problems in Hypersonic Flow." Aeronautics and Astronautics, Pergamon Press, New York, New York, 1960, pp. 344-377.

3. Zakkay, V. and Krause, E. "Boundary Conditions at the Outer Edge of the Boundary Layer on Blunted Conical Bodies." Report ARL 62-386, 1962. See also AIAA J., Vol. 1, 1963, pp. 1671-1672.

4. Wilson, R. E. "Laminar Boundary Layer Growth at Hypersonic Speeds." J. Spacecraft and Rockets, Vol. 2, 1965, pp. 490-496.

5. Rotta, N. R. and Zakkay, V. "Effects of Nose Bluntness on the Boundary Layer Characteristics of Conical Bodies at Hypersonic Speeds." NYU Report No. AA-66-66, 1966. See also Astronautica Acta., Vol. 13, 1968, pp. 507-516.

6. Murzinov, I. N. "Laminar Boundary Layer on Blunt Bodies, Allowing for Vorticity of the External Stream." NASA TT F-11007, June 1966.

7. Levine, J. N. "Finite Difference Solution of the Laminar Boundary Layer Equations Including Second-Order Effects." AIAA Paper 68-739 presented at the AIAA Fluid and Plasma Dynamics Conference, Los Angeles, California, 1968.

8. Van Dyke, M. "Second-Order Compressible Boundary-Layer Theory with Application to Blunt Bodies in Hypersonic Flow." Hypersonic Flow Research, edited by F. R. Riddell, Academic Press, Inc., 1962, pp. 37-76.

9. Adams, J. C., Jr. "Higher Order Boundary-Layer Effects on Analytic Bodies of Revolution." AEDC-TR-68-57 (AD667523), April 1968.

10. Davis, R. T. and Flügge-Lotz, I. "Laminar Compressible Flow Past Axisymmetric Blunt Bodies (Results of Second-Order Theory)." Stanford University Division of Engineering Mechanics TR-143, 1963.

11. Fannelop, T. K. and Flügge-Lotz, I. "Two-Dimensional Viscous Hypersonic Flow over Simple Blunt Bodies Including Second-Order Effects." Stanford University Division of Engineering Mechanics TR-144, 1964.

12. Maslen, S. H. "Second-Order Effects in Laminar Boundary Layers." AIAA J., Vol. 1, 1963, pp. 33-40.

13. Marchand, E. O., Lewis, C. H., and Davis, R. T. "Second-Order Boundary-Layer Effects on a Slender Blunt Cone at Hypersonic Conditions." AIAA Paper 68-54 presented at the AIAA 6th Aerospace Sciences Meeting, New York, 1968.

14. Lewis, C. H. "Comparison of a First-Order Treatment of Higher-Order Boundary Layer Effects with Second-Order Theory and Experimental Data." AEDC-TR-68-148 (AD676003), 1968.

15. Cheng, H. K. "The Blunt-Body Problem in Hypersonic Flow at Low Reynolds Number." CAL AF-1285-A-10, 1963. See also IAS Paper 63-92 presented at the IAS 31st Annual Meeting, New York, 1963.

16. Davis, R. T. "The Hypersonic Fully Viscous Shock-Layer Problem." Report SC-RR-68-840, Sandia Corporation, Albuquerque, New Mexico, 1968. See also AIAA J., Vol. 8, No. 5, May 1970, pp. 843-851.

17. Flügge-Lotz, I. and Blotter, F. G. "Computations of the Compressible Laminar Boundary-Layer Flow Including Displacement Thickness Interaction Using Finite-Difference Methods." Stanford University Division of Engineering Mechanics TR-131, 1962.

18. Patankar, S. V. and Spalding, D. B. "A Finite-Difference Procedure for Solving the Equations of the Two-Dimensional Boundary Layer." Int. J. of Heat and Mass Transfer, Vol. 10, 1967, pp. 1389-1411.

19.  Patankar, S. V. and Spalding, D. B.  Heat and Mass Transfer in Boundary Layers.  CRC Press, Cleveland, 1968.

20.  Inouye, M., Rakich, J. V., and Lomax, H.  "A Description of Numerical Methods and Computer Programs for Two-Dimensional and Axisymmetric Flow Over Blunt-Nosed and Flared Bodies."  NASA TN D-2970, August 1965.

21.  Mayne, A. W., Jr. and Dyer, D. F.  "Comparisons of Theory and Experiment for Turbulent Boundary Layers on Simple Shapes at Hypersonic Conditions."  Proceedings of the 1970 Heat Transfer and Fluid Mechanics Institute, Stanford University Press, June 1970, pp. 168-188.

22.  Whitfield, J. D. and Griffith, B. J.  "Hypersonic Viscous Drag Effects on Blunt Slender Cones."  AIAA J., Vol. 2, 1964, pp. 1714-1722.

23.  Lewis, C. H. and Whitfield, J. D.  "Theoretical and Experimental Studies of Hypersonic Viscous Effects."  AEDC-TR-65-100 (AD462717), May 1965.  Also AGARDograph 97, Part III, 1965, pp. 63-119.

**APPENDIX**
**ILLUSTRATIONS**
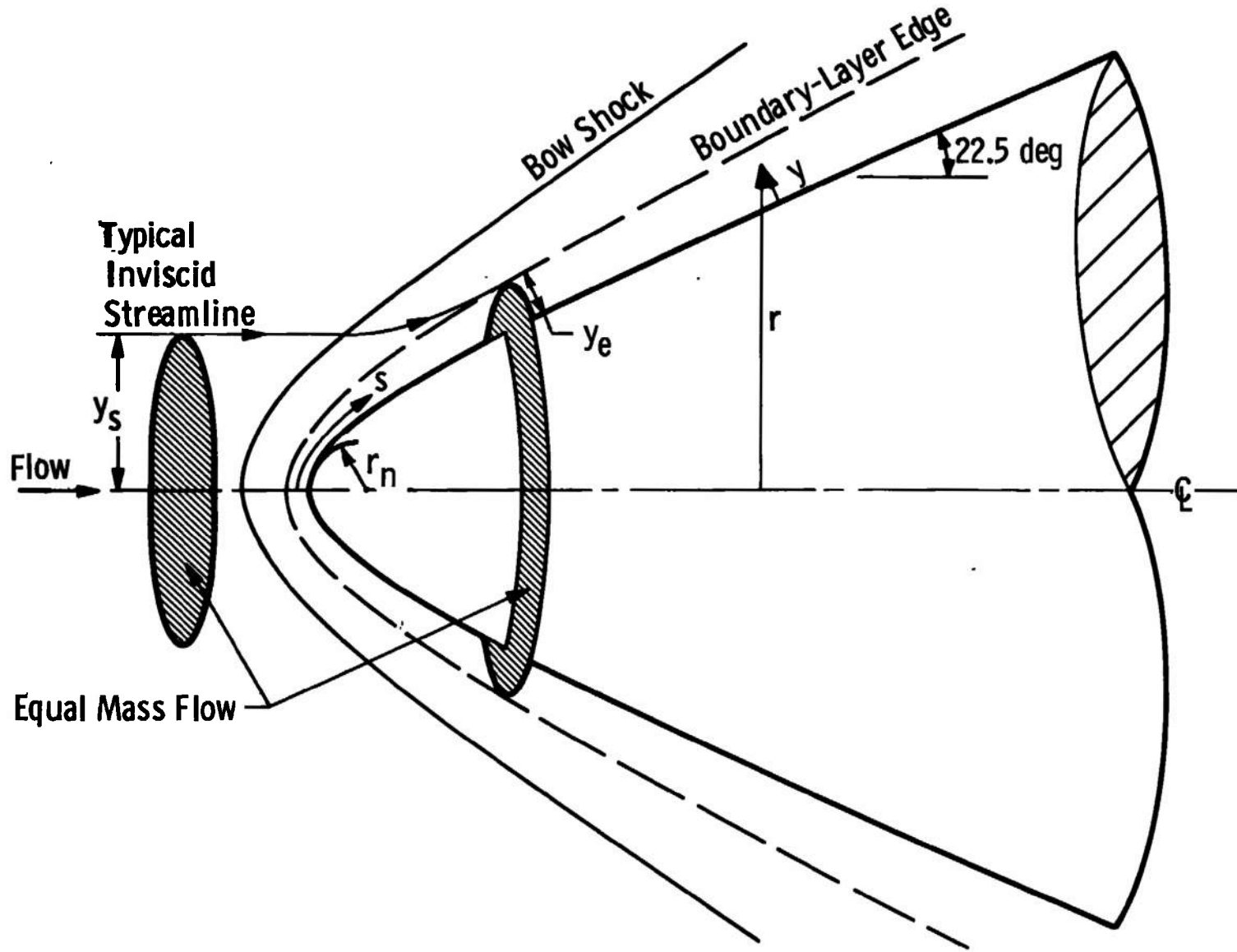
Fig. 1 Hyperboloid Geometry, Showing Inviscid Streamline Swallowing
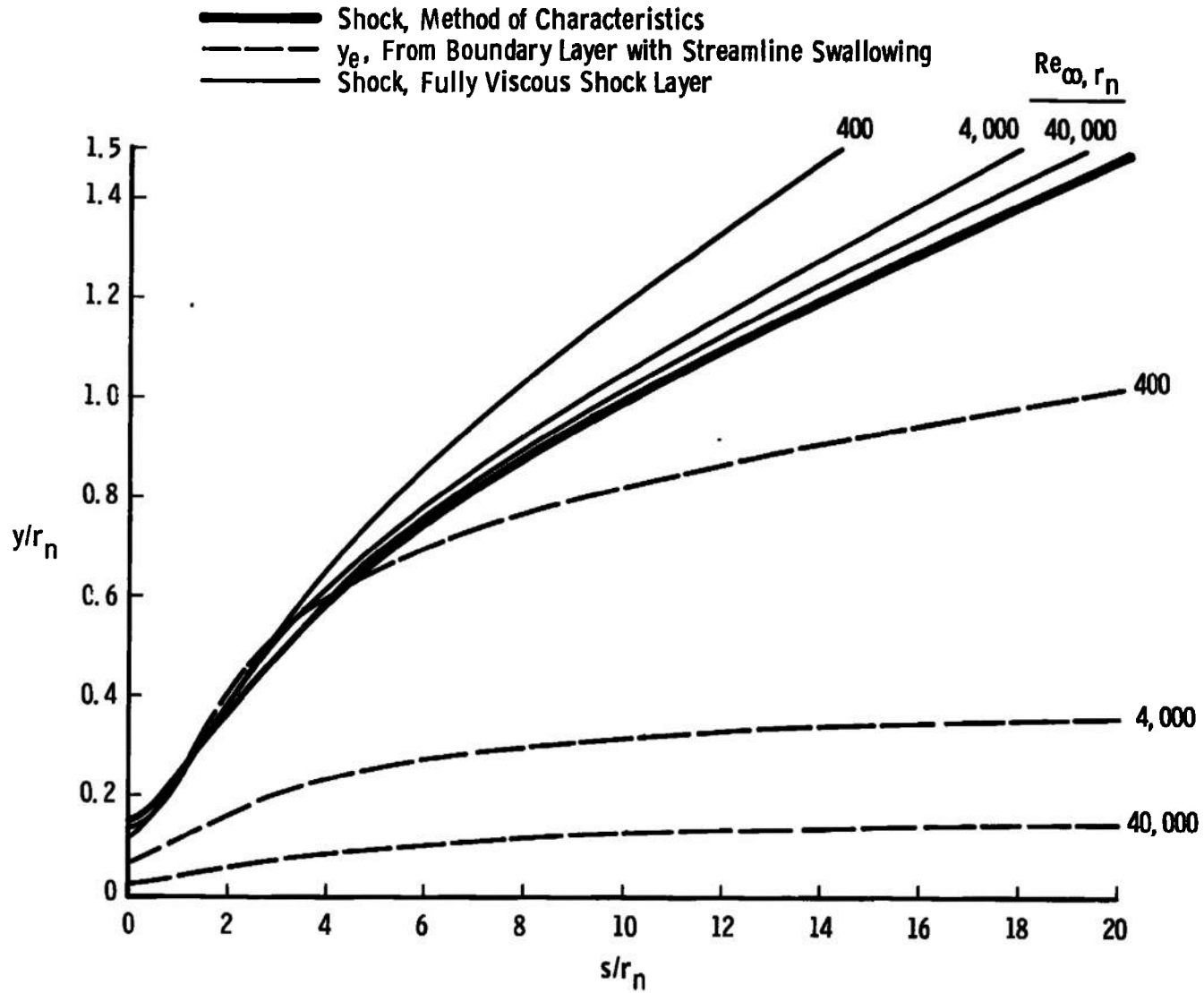
Fig. 2  Thickness of Boundary Layer, Shock Layer, and Inviscid Flow Field

Fully Viscous Shock Layer
Boundary Layer with Streamline Swallowing

$St_\infty$

Second-Order Boundary Layer

Boundary Layer without Streamline Swallowing

$s/r_n$
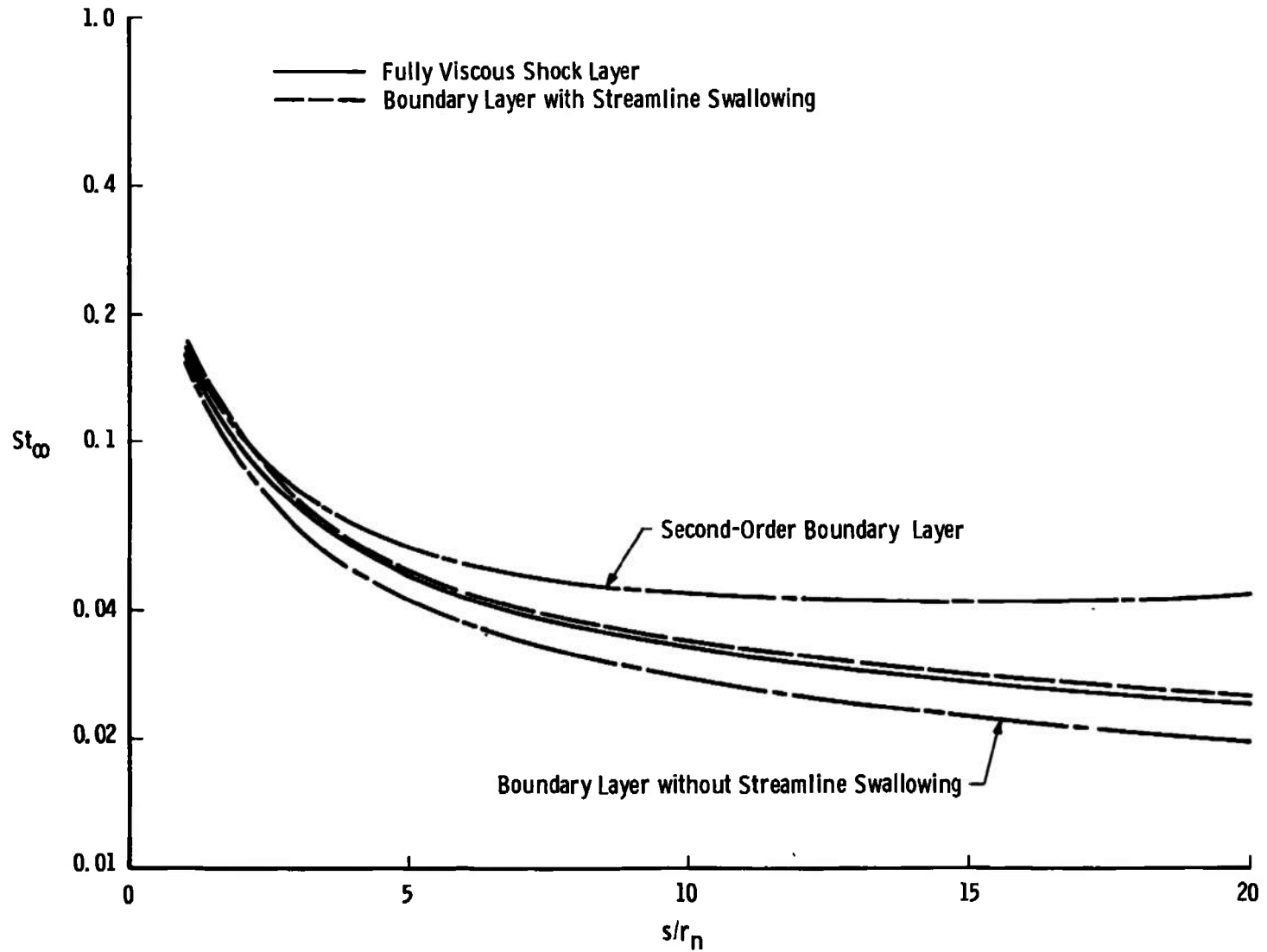
Fig. 3 Stanton Number Distribution for $Re_{\infty, r_n} = 400$
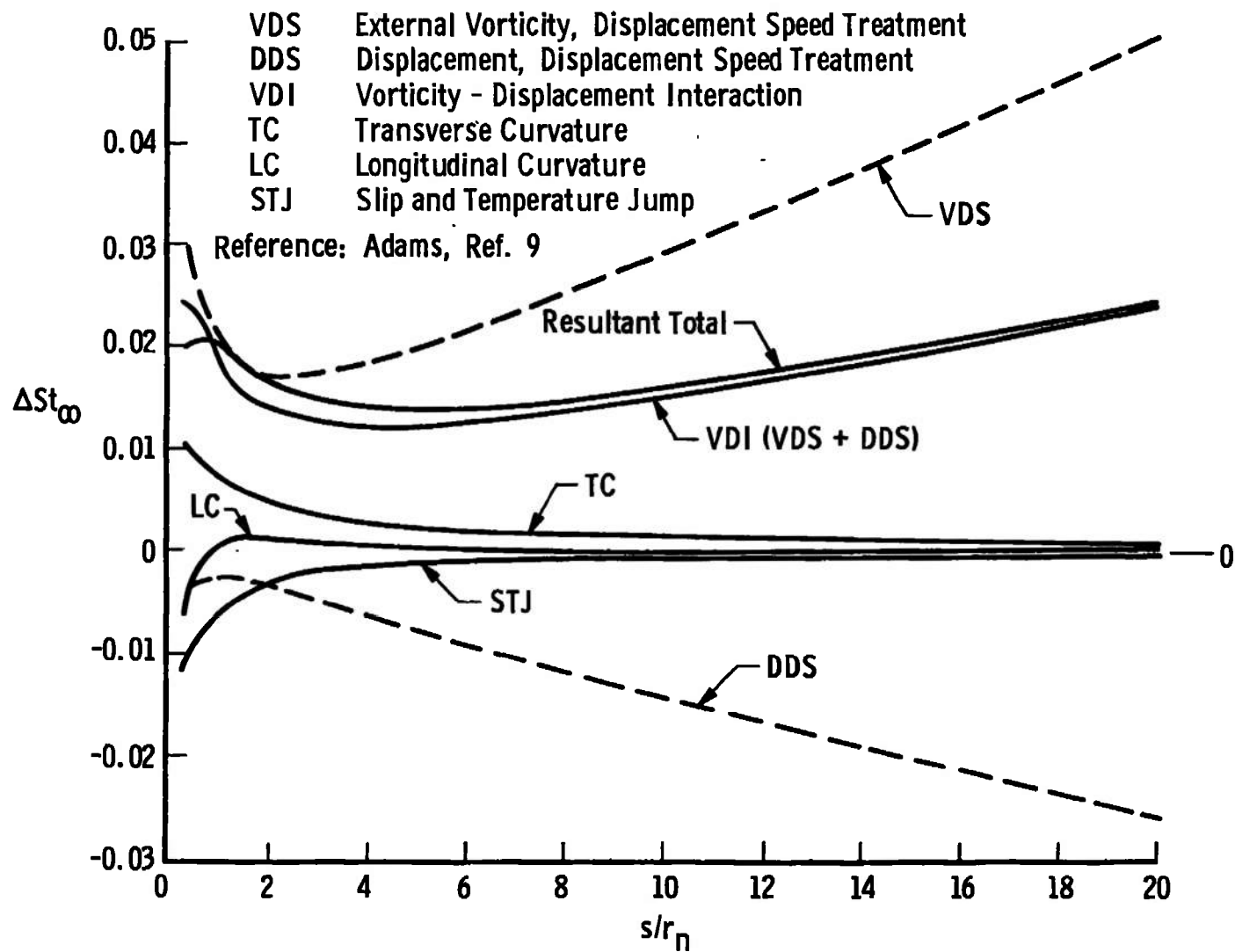
Fig. 4 Increment in Stanton Number Because of Second-Order Effects, $Re_{\infty, r_n} = 400$
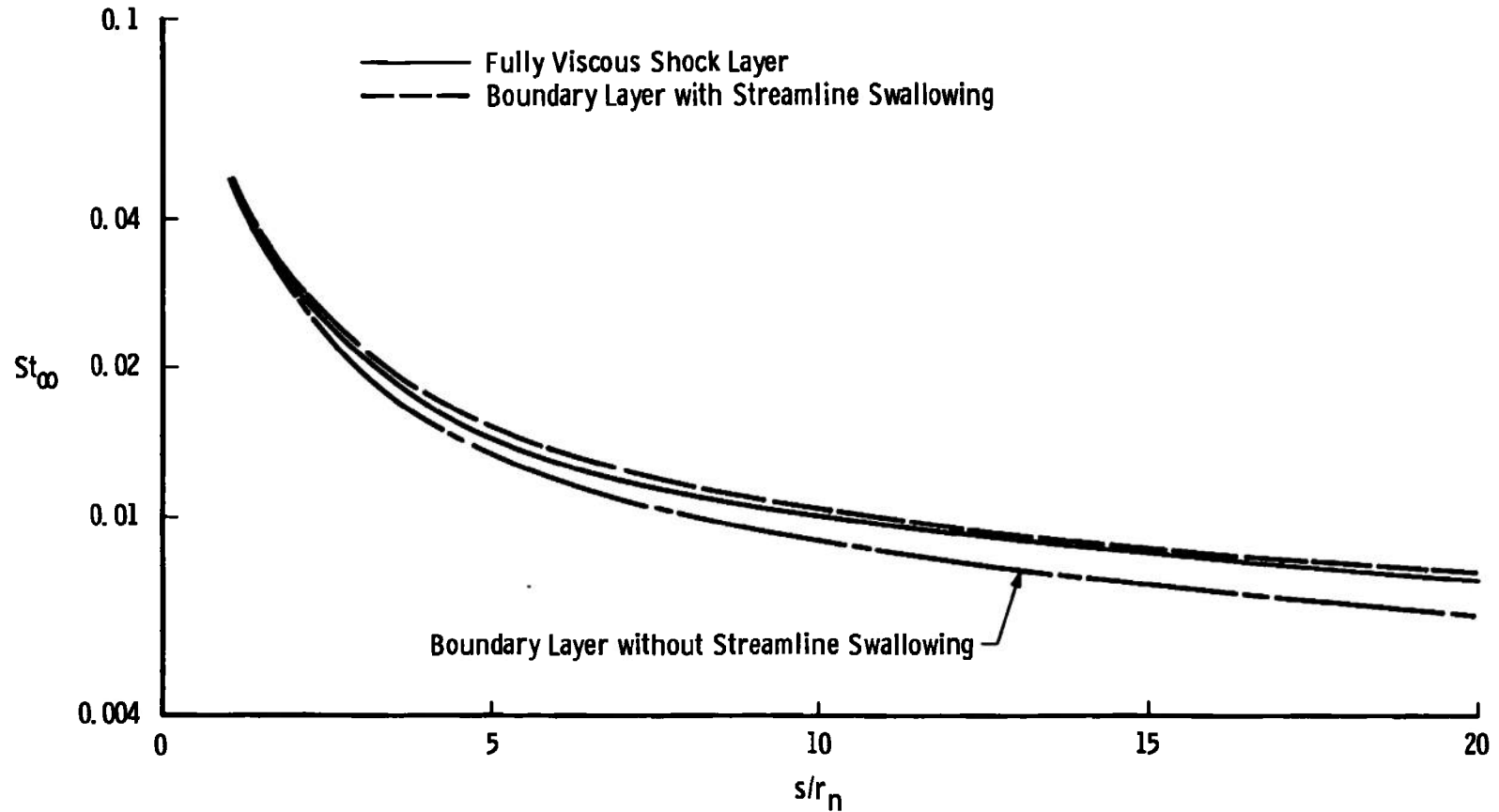
Fig. 5 Stanton Number Distribution for $Re_{\infty, r_n} = 4000$
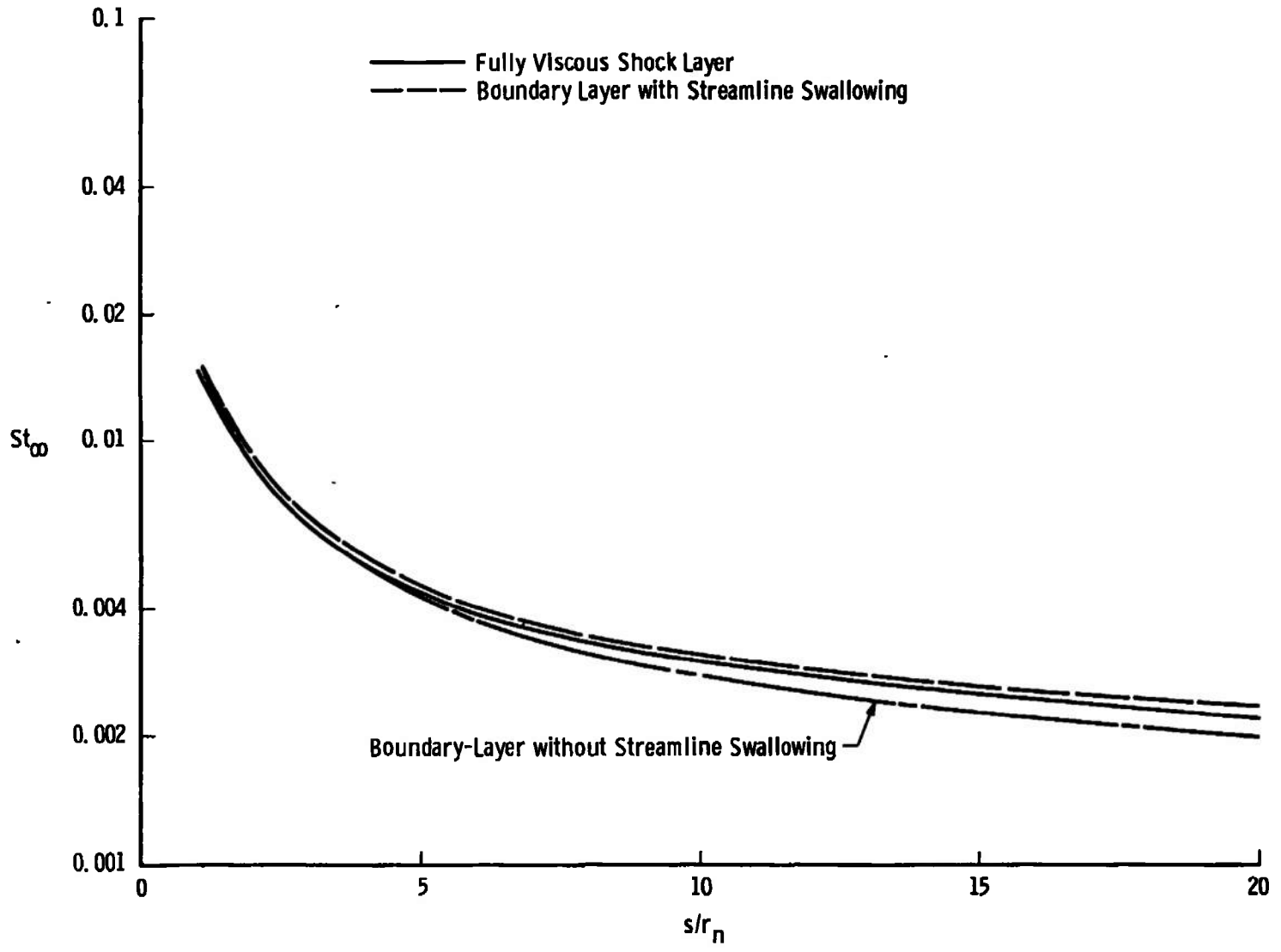
Fig. 6 Stanton Number Distribution for $Re_{\infty,r_n} = 40,000$
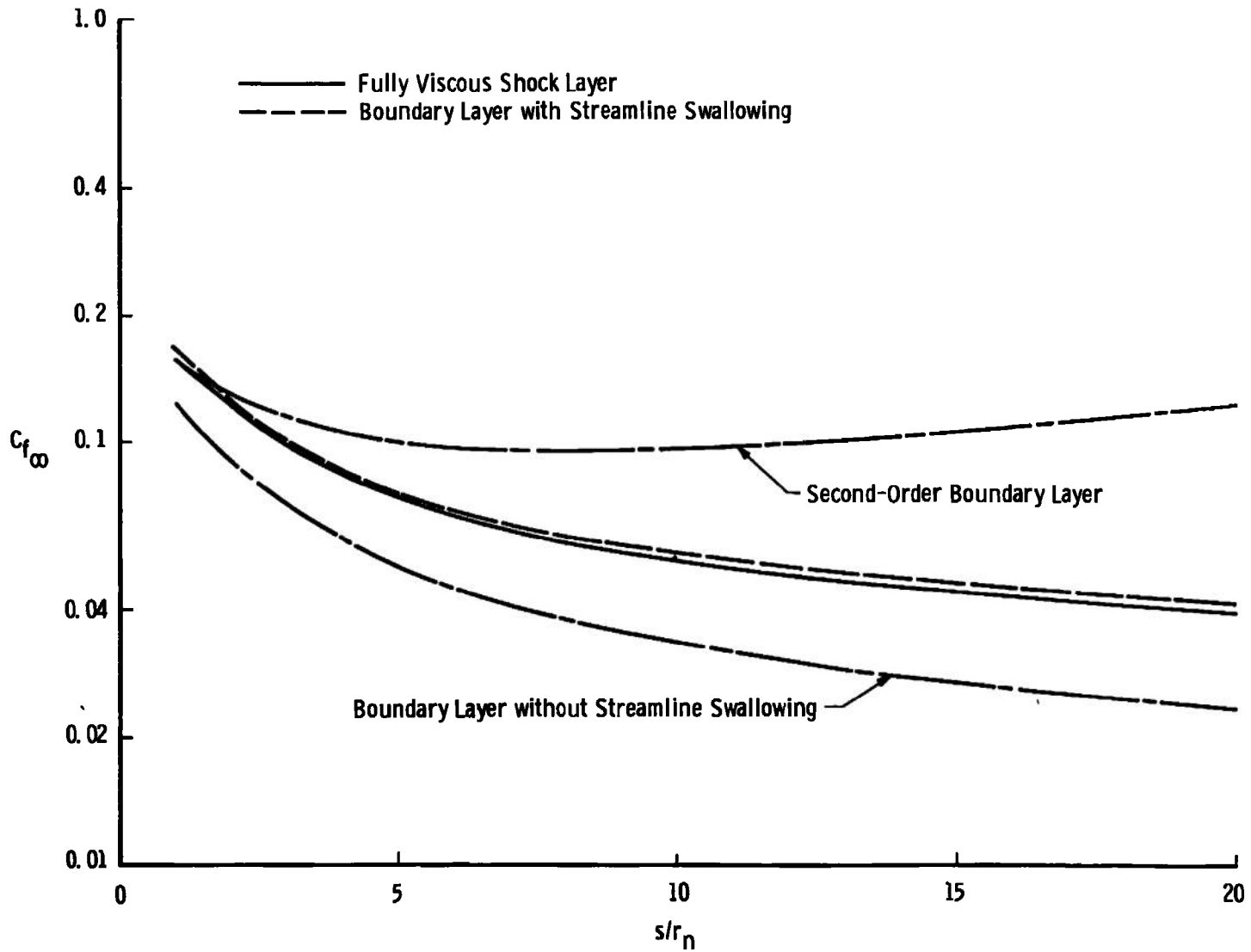
Fig. 7  Local Skin-Friction Coefficient Distribution for $Re_{\infty, r_n} = 400$
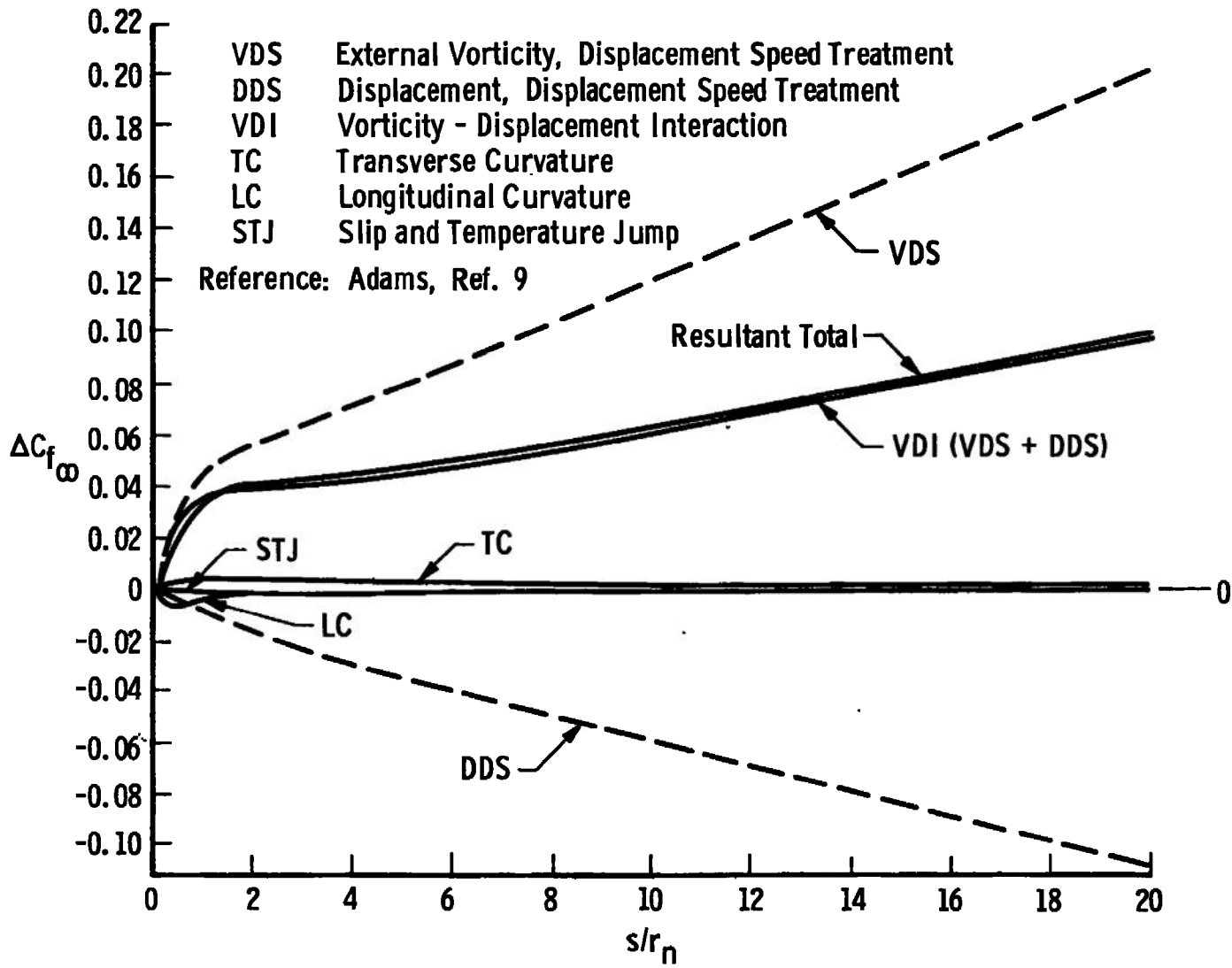
Fig. 8  Increment in Local Skin-Friction Coefficient Because of Second-Order Effects,  $Re_{\infty,r_n} = 400$
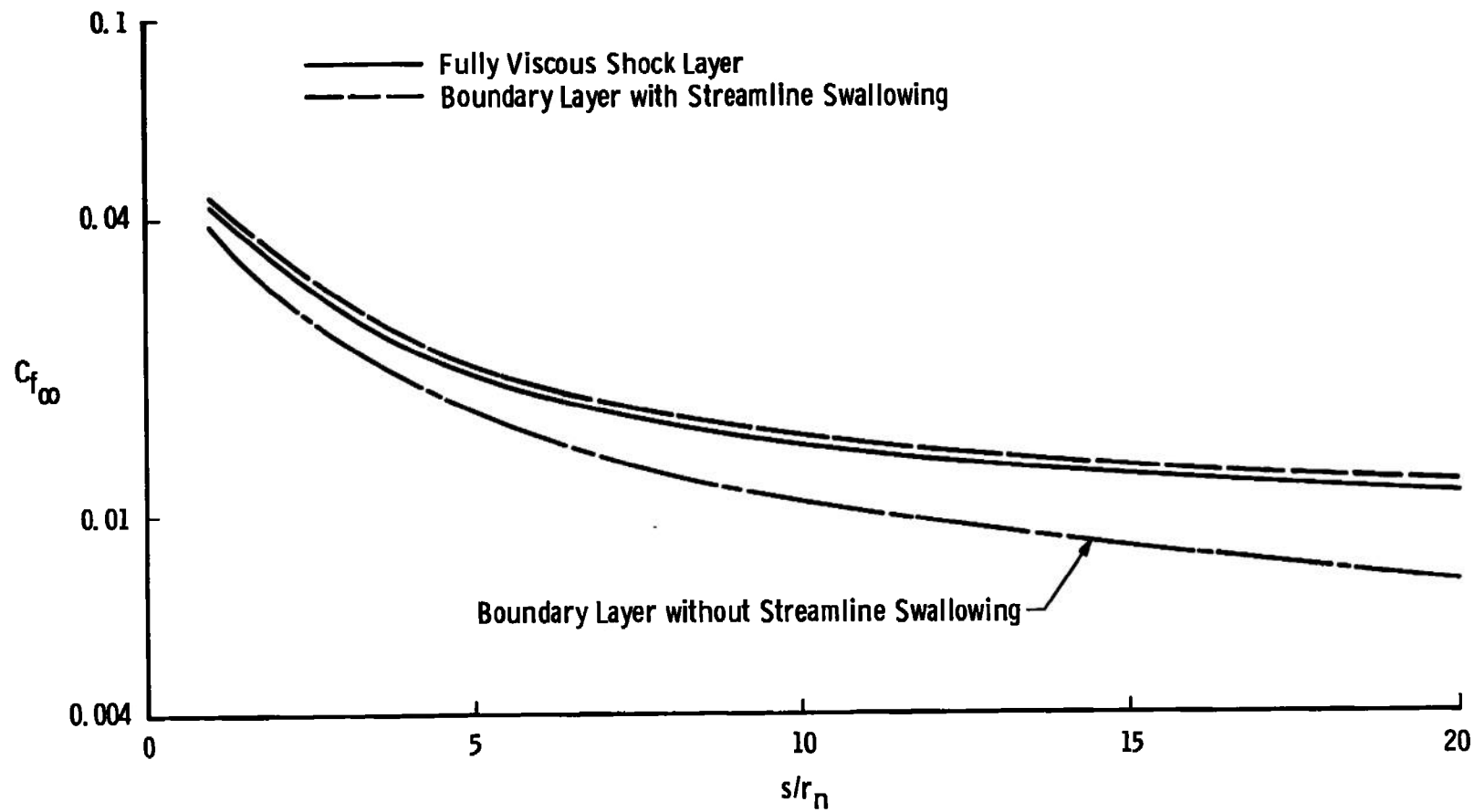
**Fig. 9  Local Skin-Friction Coefficient Distribution for $Re_{\infty, r_n} = 4000$**
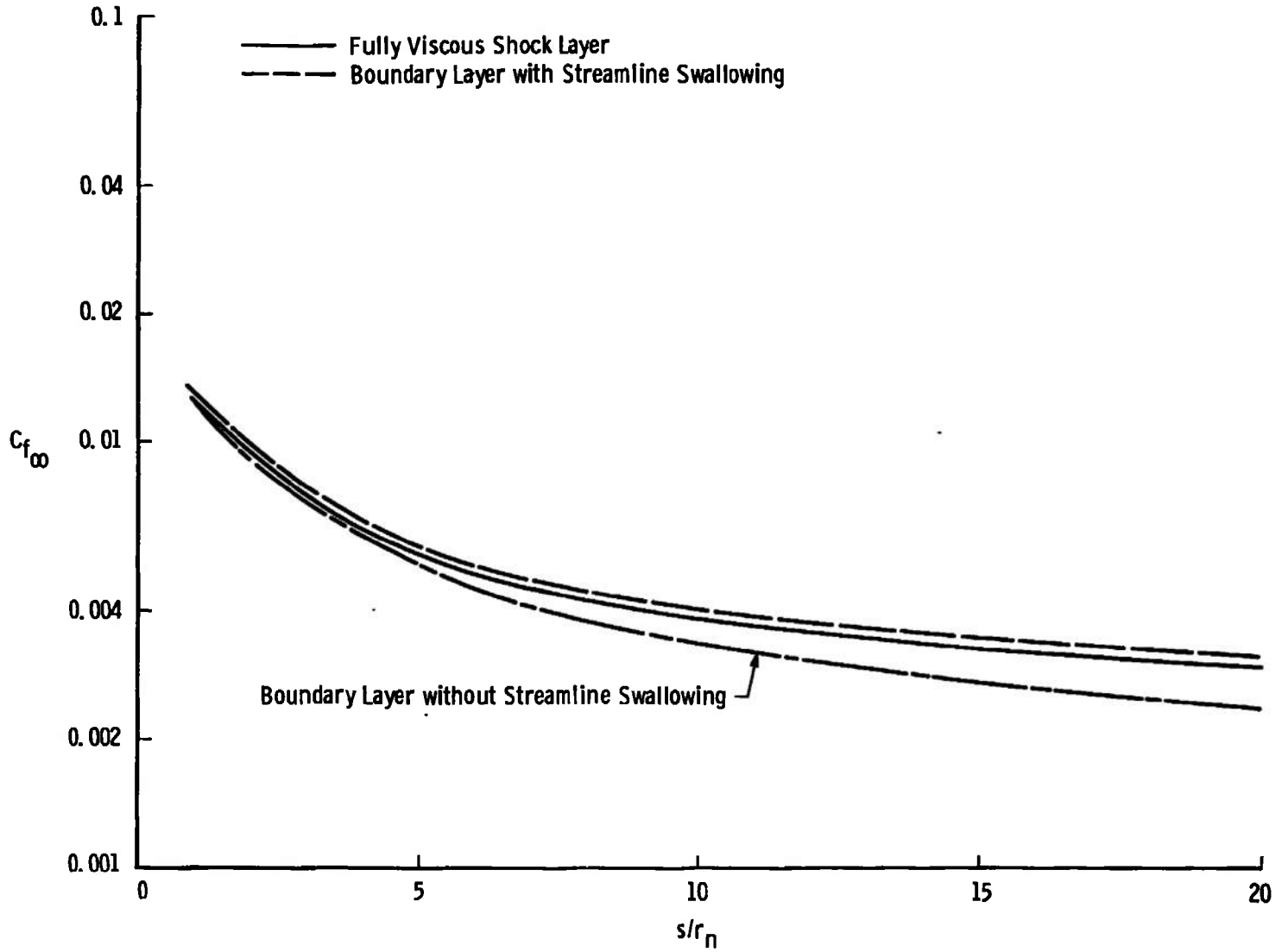
Fig. 10  Local Skin-Friction Coefficient Distribution for $Re_{\infty, r_n} = 40,000$
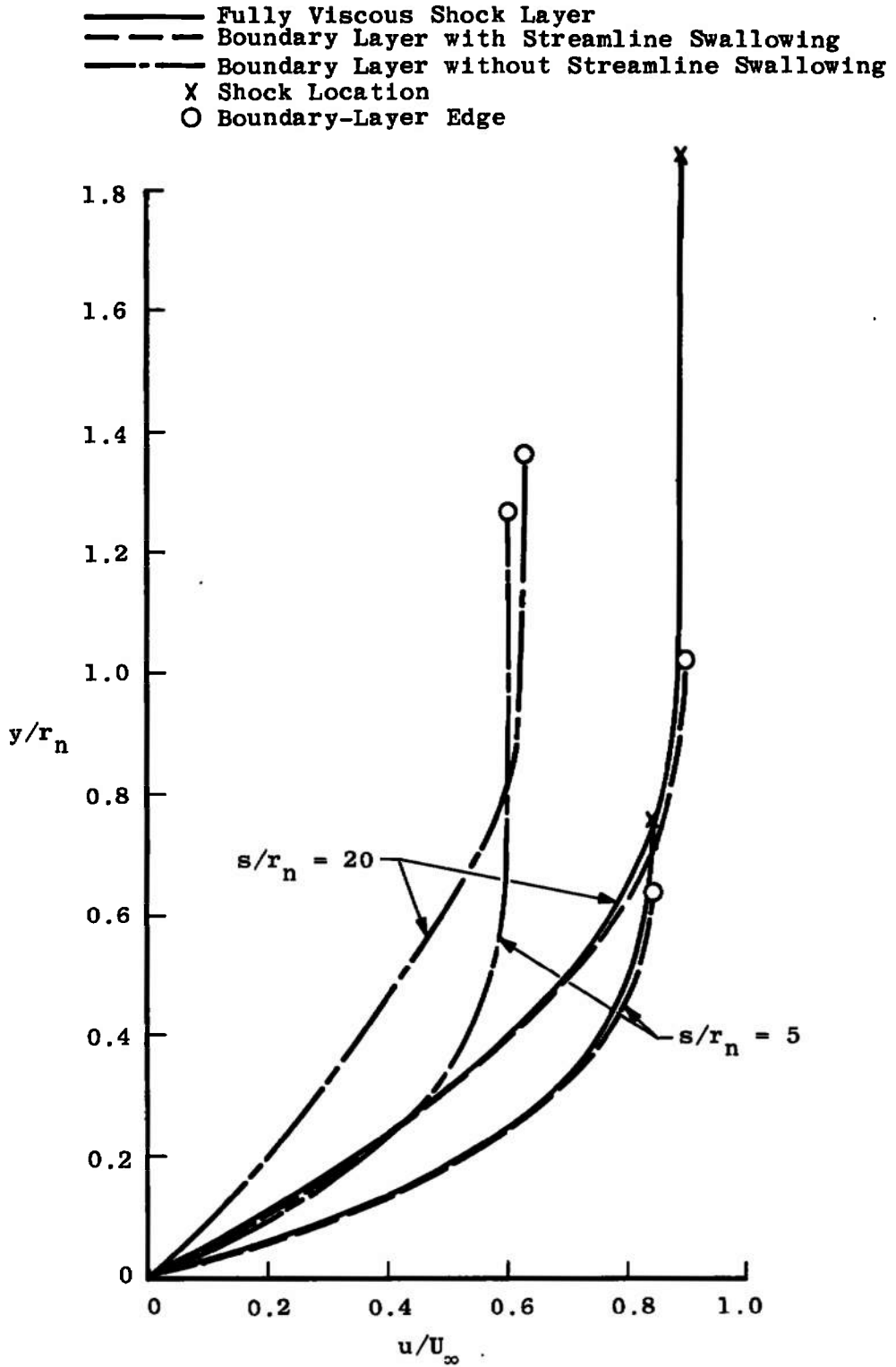
Fig. 11 Velocity Profiles for $Re_{\infty,r_n} = 400$
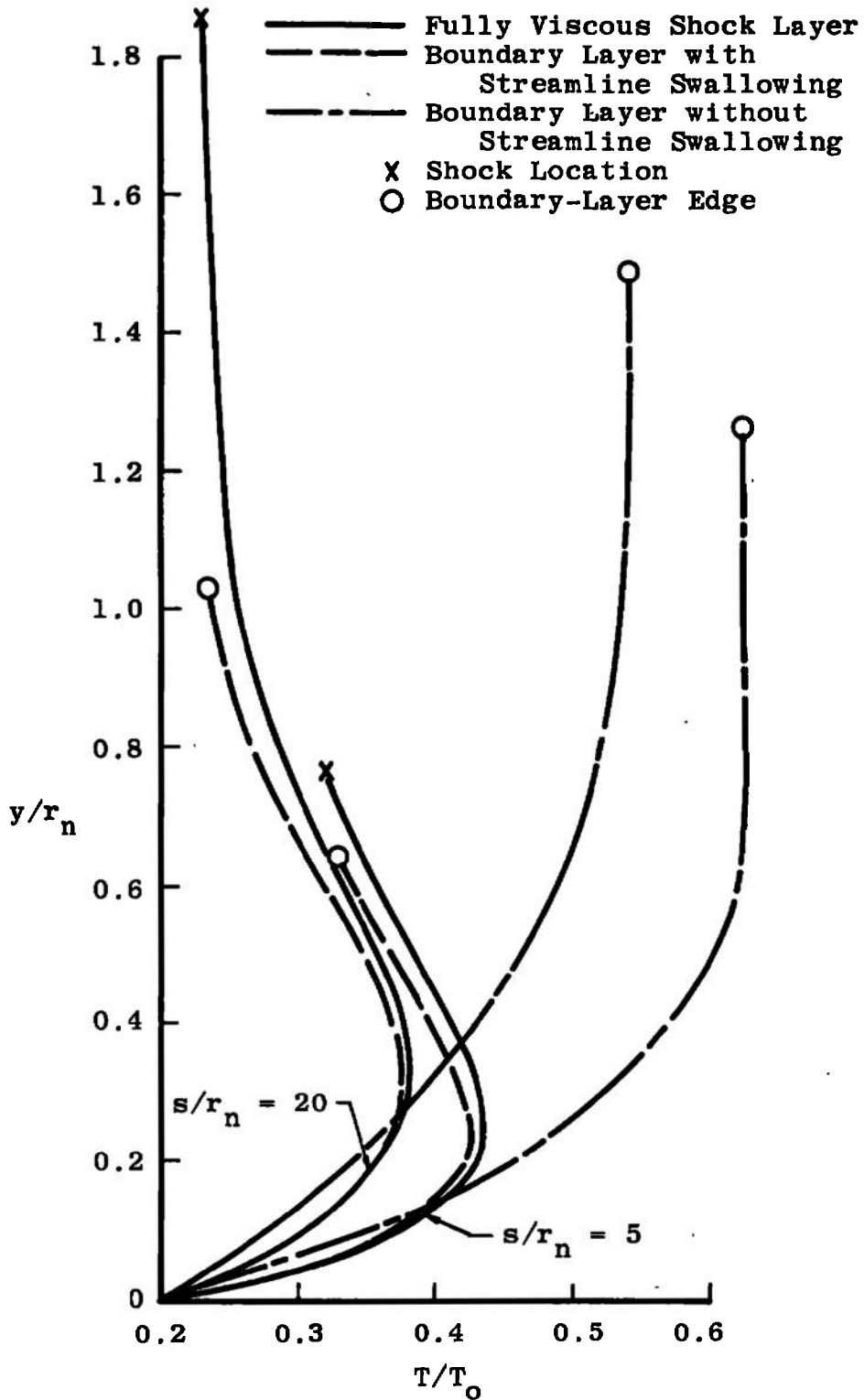
Fig. 12 Temperature Profiles for $Re_{\infty, r_n} = 400$
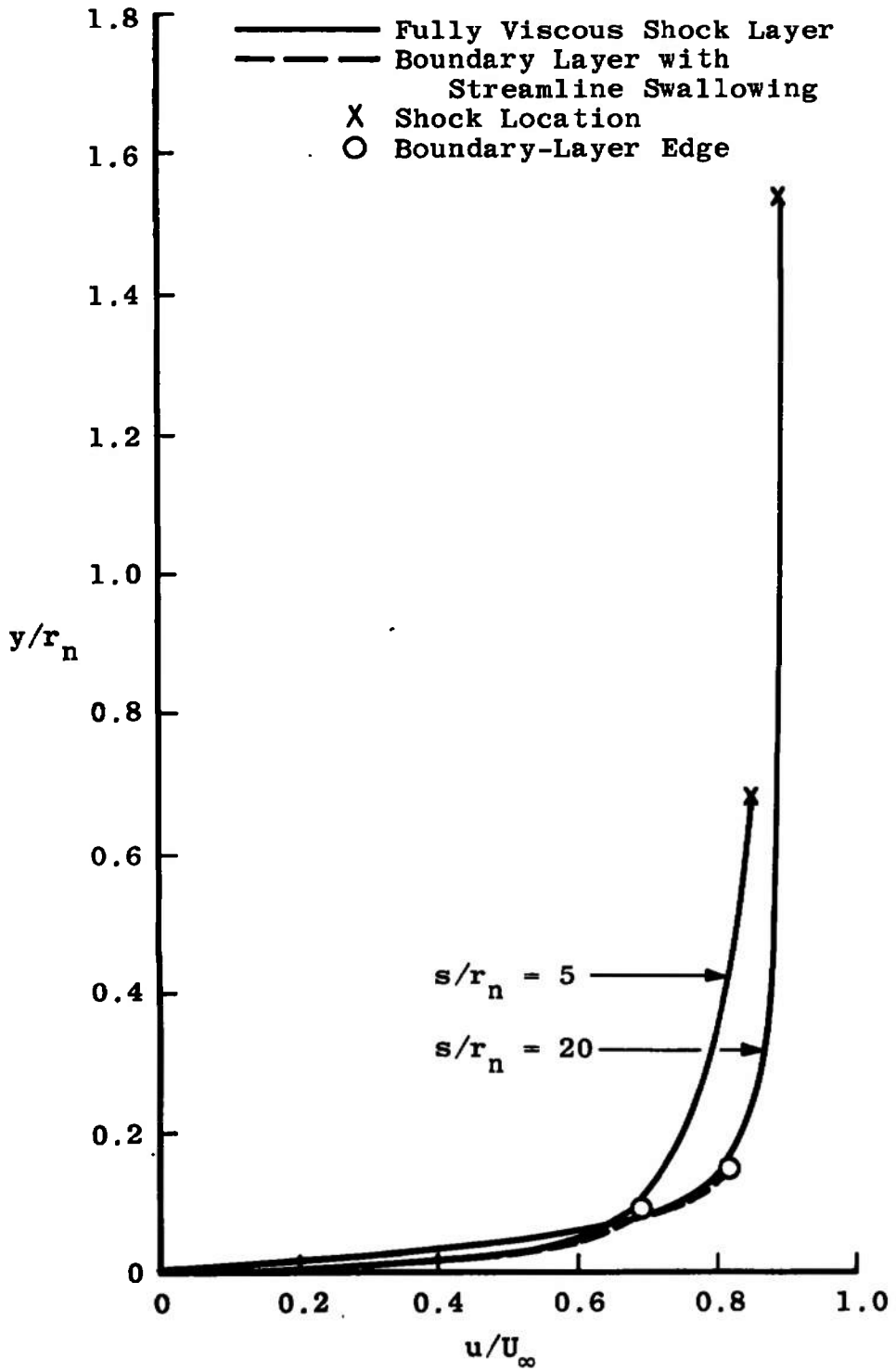
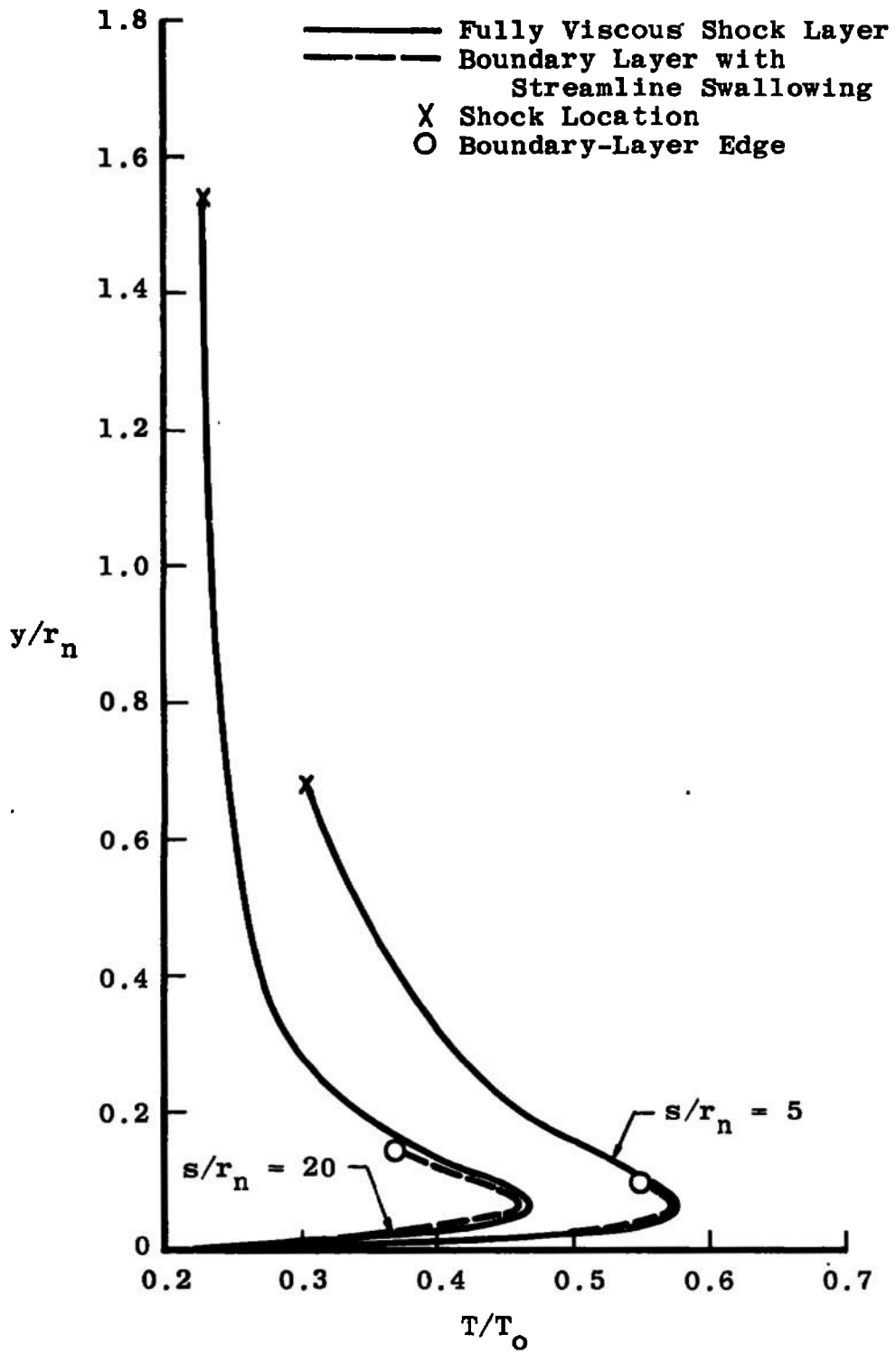Fig. 13 Velocity Profiles for $Re_{\infty,r_n} = 40,000$

Fig. 14 Temperature Profiles for $Re_{\infty,r_n} = 40,000$
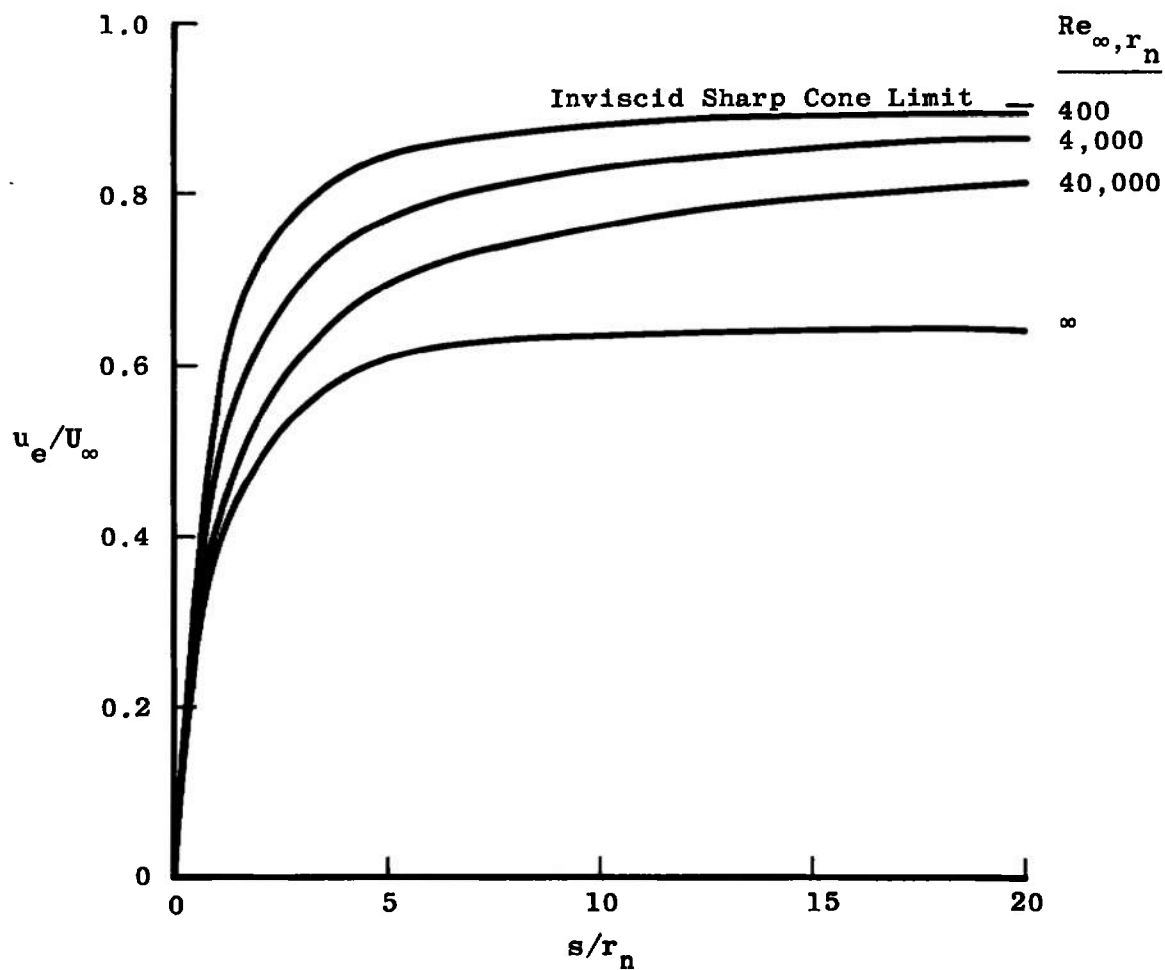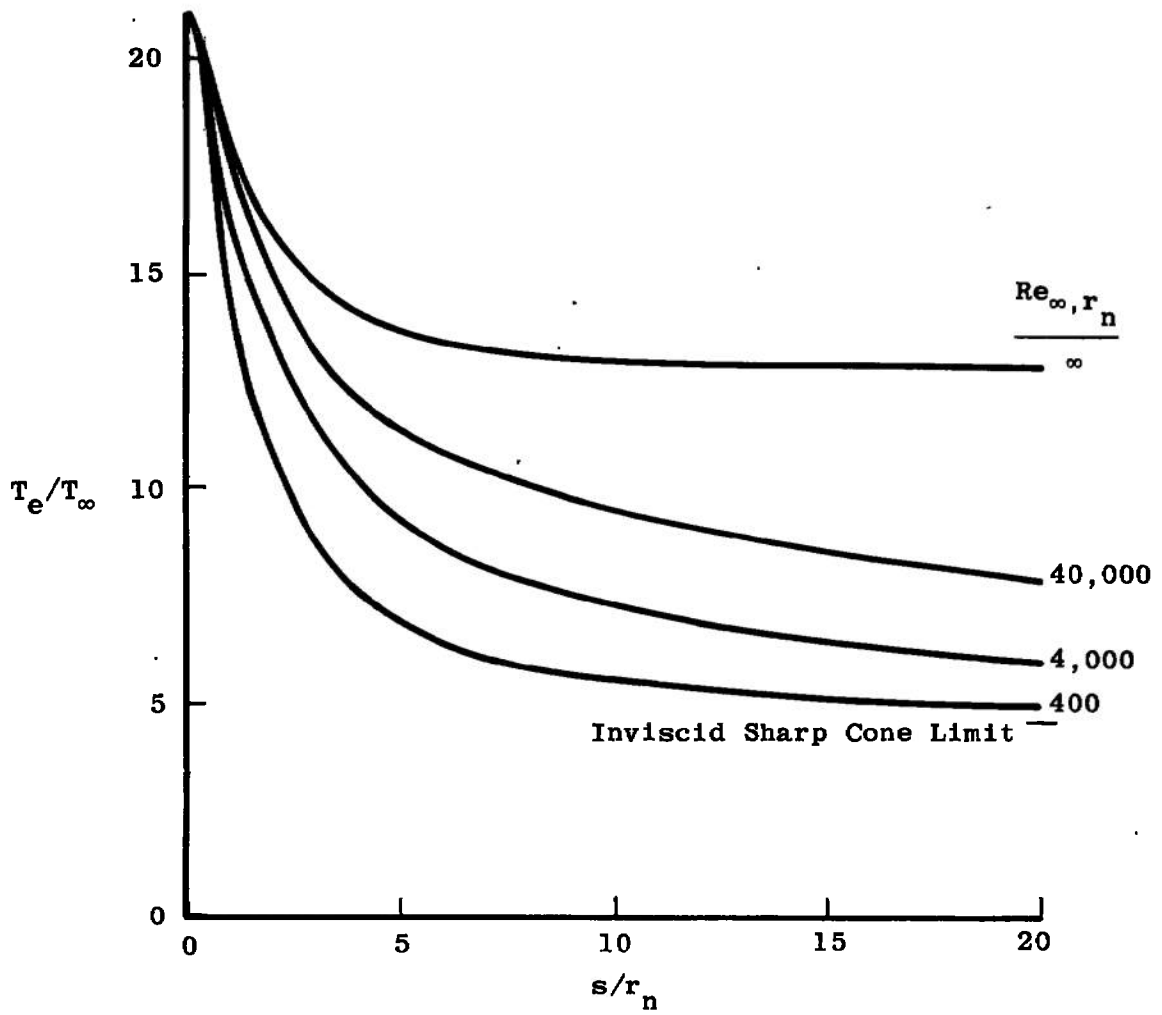
Fig. 15 Outer Edge Velocity Distribution
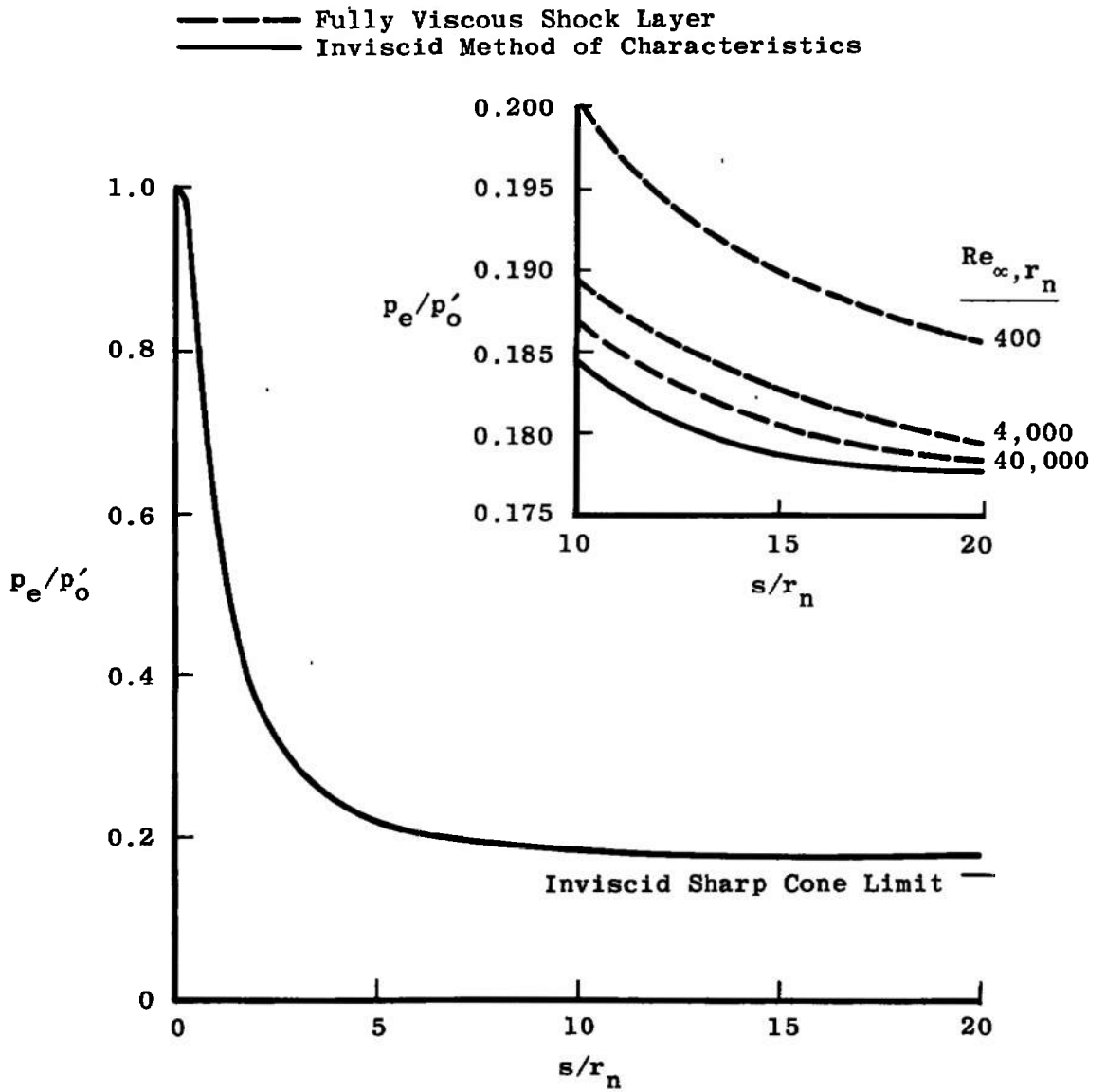
Fig. 16 Outer Edge Temperature Distribution

Fig. 17 Surface Pressure Distribution

Fig. 18 Pressure Profiles
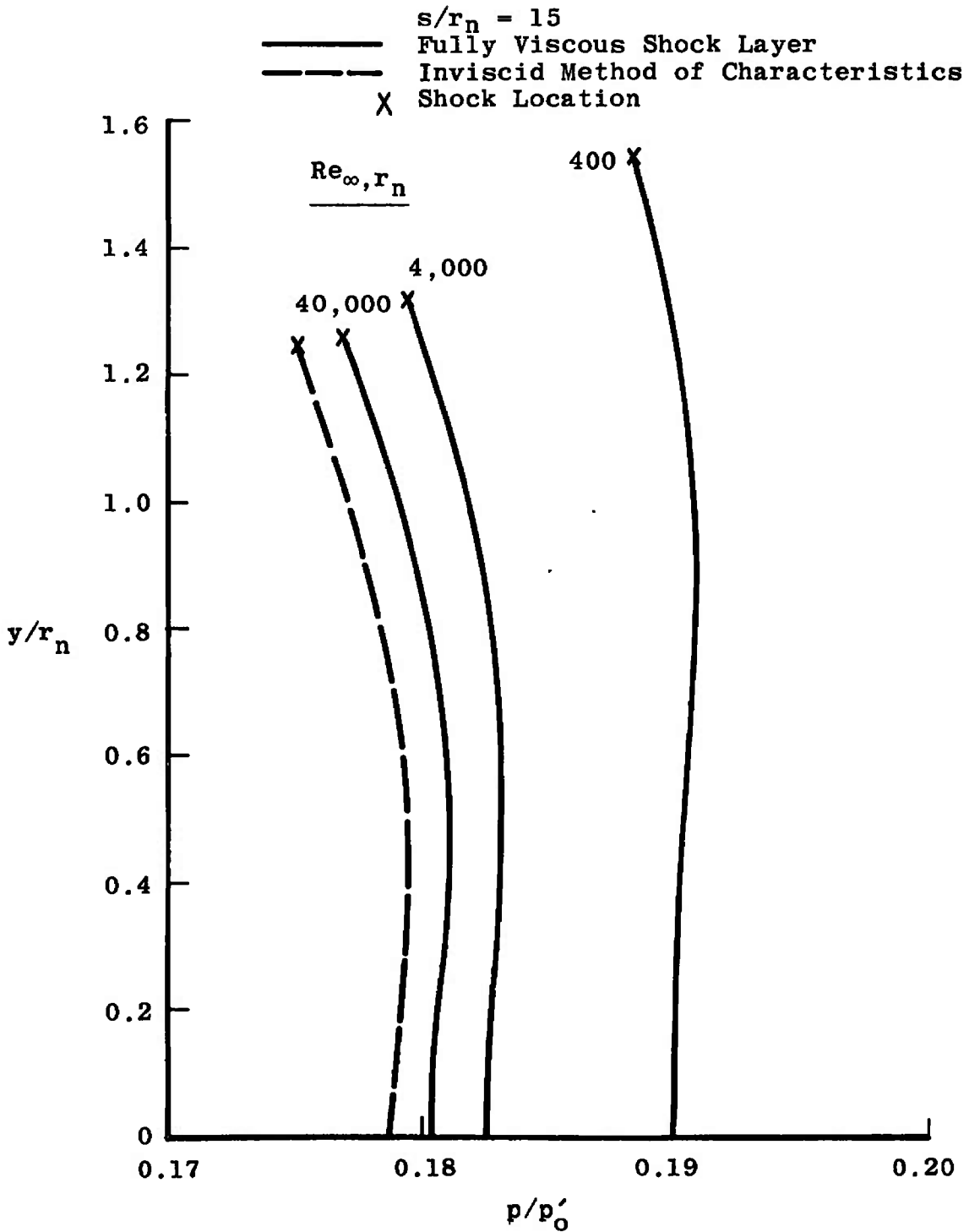
| DOCUMENT CONTROL DATA - R & D | | |
|---|---|---|
| (Security classification of title, body of abstract and indexing annotation must be entered when the overall report is classified) | | |

| 1. ORIGINATING ACTIVITY (Corporate author) | 2a. REPORT SECURITY CLASSIFICATION |
|---|---|
| Arnold Engineering Development Center ARO, Inc., Operating Contractor Arnold Air Force Station, Tennessee 37389 | UNCLASSIFIED |
| | 2b. GROUP  N/A |

**3. REPORT TITLE**

STREAMLINE SWALLOWING BY LAMINAR BOUNDARY LAYERS
IN HYPERSONIC FLOW

**4. DESCRIPTIVE NOTES** *(Type of report and inclusive dates)*

Final Report    September 1969 to June 1970

**5. AUTHOR(S)** *(First name, middle initial, last name)*

A. W. Mayne, Jr. and J. C. Adams, Jr., ARO, Inc.

| 6. REPORT DATE | 7a. TOTAL NO. OF PAGES | 7b. NO. OF REFS |
|---|---|---|
| March 1971 | 43 | 23 |

| 8a. CONTRACT OR GRANT NO.  F40600-71-C-0002 | 9a. ORIGINATOR'S REPORT NUMBER(S) |
|---|---|
| b. PROJECT NO. 8953 | AEDC-TR-71-32 |
| c. Program Element 62201F | 9b. OTHER REPORT NO(S) (Any other numbers that may be assigned this report) |
| d. Task 03 | ARO-VKF-TR-70-329 |

**10. DISTRIBUTION STATEMENT**

This document has been approved for public release and sale;
its distribution is unlimited.

| 11. SUPPLEMENTARY NOTES | 12. SPONSORING MILITARY ACTIVITY |
|---|---|
| Available in DDC. | Arnold Engineering Development Center, AFSC, Arnold Air Force Station, Tennessee 37389 |

**13. ABSTRACT**

Flow over a cold-wall, 22.5-deg asymptotic half-angle hyperboloid at a free-stream Mach number of 10 and free-stream Reynolds numbers (based on nose radius) of 400, 4000, and 40,000 is considered. Numerical results from a streamline-swallowing, nonsimilar, laminar, boundary-layer analysis are compared with results from classical boundary-layer theory, second-order boundary-layer theory, and a fully viscous shock-layer analysis; the results of the latter are used as a standard of comparison. The major improvement effected by the streamline-swallowing analysis is the inclusion of shock curvature effects on the boundary conditions applied along the outer edge of the boundary layer. Results from the streamline-swallowing boundary-layer analysis agree well with the results of the fully viscous shock-layer analysis, but the classical boundary layer and the second-order boundary-layer results give poor agreement. Reasons for the success of the one method and the failure of the other two are discussed.

**DD** FORM NOV 65 **1473**

| 14. KEY WORDS | LINK A | | LINK B | | LINK C | |
|---|---|---|---|---|---|---|
| | ROLE | WT | ROLE | WT | ROLE | WT |
| boundary layers | | | | | | |
| hypersonic flow | | | | | | |
| laminar flow | | | | | | |